RSC Advances

PAPER

View Article Online
View Journal | View Issue

Cite this: *RSC Adv.*, 2017, **7**, 7003

High-quality $K_{0.47}Na_{0.53}NbO_3$ single crystal toward high performance transducer

Chengpeng Hu,[a] Hao Tian,*[a] Xiangda Meng,[a] Guang Shi,[a] Wenwu Cao[b] and Zhongxiang Zhou*[a]

Received 30th November 2016
Accepted 7th January 2017

DOI: 10.1039/c6ra27546j

www.rsc.org/advances

A large-sized, high-quality single crystal of $K_{0.47}Na_{0.53}NbO_3$ was grown by the top-seeded solution growth method. A complete set of elastic, dielectric, and piezoelectric constants for a $[001]_C$-poled $K_{0.47}Na_{0.53}NbO_3$ single crystal was determined *via* combined resonance and ultrasonic methods. The $[001]_C$-poled $K_{0.47}Na_{0.53}NbO_3$ (KNN47) single crystal exhibits a large piezoelectric coefficient (d_{33} = 220 pC N^{-1}), high coupling coefficients (k_{33} = 0.759 and k_t = 0.702), high dielectric constants (ε_{11}^T = 2194 and ε_{11}^S = 2162), and relatively high elastic compliance constants (S_{11}^E = 14.3 × 10^{-12} N m^{-2} and S_{33}^E = 17.6 × 10^{-12} N m^{-2}). Furthermore, a large electrical field induced strain of 0.16% was measured from the slope in the unipolar strain *versus* electric field dependence. The piezoelectric coefficient, d_{33}^*, was determined to be as high as 401 pm V^{-1}, likely resulting due to the morphotropic phase boundary around x = 0.5. These excellent properties make KNN47 a good candidate for application as a high-performance transducer material.

Introduction

Despite the favorable properties of lead-based piezoelectric materials, research on alternative lead-free piezoelectric materials has attracted a lot of attention over the last decade in order to mitigate concerns over the environmental and health effects of lead-based products in the atmosphere.[1–4] Among these lead-free piezoelectric materials, potassium sodium niobate (K_x-$Na_{1-x}NbO_3$, referred to as KNNx%) based materials are one of the most promising classes for real-world applications due to their relatively good piezoelectric response and high Curie temperature (T_C = 415 °C of KNN50)[5] compared with other lead-free materials, such as barium titanate.[6–8] However, studying the nature of KNN materials in ceramics is more challenging than similar studies on single crystals because of the presence of grain boundaries in ceramics.[9]

Among the pure KNN materials, the composition of potassium sodium niobate with x = 0.5 is the most interesting due to the presence of a turning point in the structural parameters,[10–12] a phase transition from rhombohedral to orthorhombic and orthorhombic to tetragonal,[12,13] and its density,[11] remanent polarization, coercive field,[14] and piezoelectric coefficient, d_{33}.[15] Nearly all studies have typically focused on the monoclinic–orthorhombic morphotropic phase boundary in KNN with x = 0.5, which differs from the orthorhombic–tetragonal polymorphic phase transition in Li and Ta doped-KNN materials. The piezoelectric constant, d_{33}, of pure KNN crystal has been reported to be as high as 160 pC N^{-1},[16,17] with a high thickness electromechanical coupling coefficient, k_t, of 0.7 in large-sized $[001]_C$-poled $Li_x(Na_{0.5}K_{0.5})_{1-x}NbO_3$ ($x \approx 0.02$) single crystals.[18] For both device design and fundamental studies, it is necessary to know the complete set of piezoelectric, dielectric and elastic properties of KNN single crystals. In order to obtain a large-sized single crystal with improved piezoelectric properties, recent years have seen significant efforts to develop more effective growth methods for larger KNN single crystals.[18,19] Comparing with the flux, Bridgman and solid-state single crystal growth methods, it is more difficult to manipulate the crystal growth through controlling the temperature and growth rate. It is more dependent on experience, but ignoring the thermal stress and nucleation problems during the crystal growth. In a previous work, we have reported a complete set of matrix properties for domain engineered KNN80 single crystals.[20] However, it has been found that high-quality, large single crystals of KNN50 are still challenging to grow due to difficulties in controlling the compositional uniformity, amongst other factors. There have been no reports of the piezoelectric, dielectric and elastic tensor properties in pure KNN crystal around the x = 0.5 boundary. The availability of a complete set of material constants for KNN80 single crystals motivates further studies to obtain a similarly complete set of data for KNN single crystals around x = 0.5.

In this study, a sufficiently large and high-quality single crystal of KNN47, with no cracks, was grown *via* the top-seeded solution growth (TSSG) method of large crucible with a mount

[a]*Department of Physics, Harbin Institute of Technology, Harbin 150001, P. R. China. E-mail: tianhao@hit.edu.cn; zhouzx@hit.edu.cn*

[b]*Materials Research Institute, The Pennsylvania State University, University Park, Pennsylvania 16802, USA*

Fig. 1 Photograph of KNN47 single crystal grown *via* TSSG.

of solution to grown relatively small crystal, as shown in Fig. 1. The dimensions of the KNN47 single crystal were 9 × 9 × 35 mm^3. For the first time, we report a full property matrix set for the $[001]_C$-poled KNN47 single crystal from measured data around the $x = 0.5$ boundary.

Experimental procedure

Powders of K_2CO_3, Na_2CO_3, and Nb_2O_5 with purities of 99.99% were used as the raw materials and were mass-weighted to obtain the composition of KNN47; excess amounts of 10% (by mole) solutions of Na_2CO_3 and K_2CO_3 were added as a self-flux. The materials were mixed in a ball mill with ethanol for 24 h, and then placed into a Pt crucible and calcined at 850 °C for 6 h. The KNN47 single crystal was then grown at 1110 °C in a medium-frequency induction furnace under an air atmosphere. The velocities of rotation and pulling of the crystal were approximately 30 rpm and 4.0 mm per day, respectively. After about 5–6 days, the crystals were cooled down to room temperature at a rate of 0.5 °C min^{-1}. The crystal structures were confirmed by X-ray diffraction (XRD) (XRD-6000, Shimadzu, Kyoto, Japan), and the strain *vs.* electric field (S–E) loop of the crystals was recorded using a ferroelectric test system (Precision Premier II, Radiant Technology, Inc., Albuquerque, NM, USA).

For the effective macroscopic symmetry with the tetragonal point group 4 mm, there are a total of 11 independent material constants: six elastic constants, three piezoelectric constants, and two dielectric constants. All samples were oriented by a Laue X-ray machine with an accuracy of ±0.5° and cut from the same slice with uniform composition and aspect ratios.

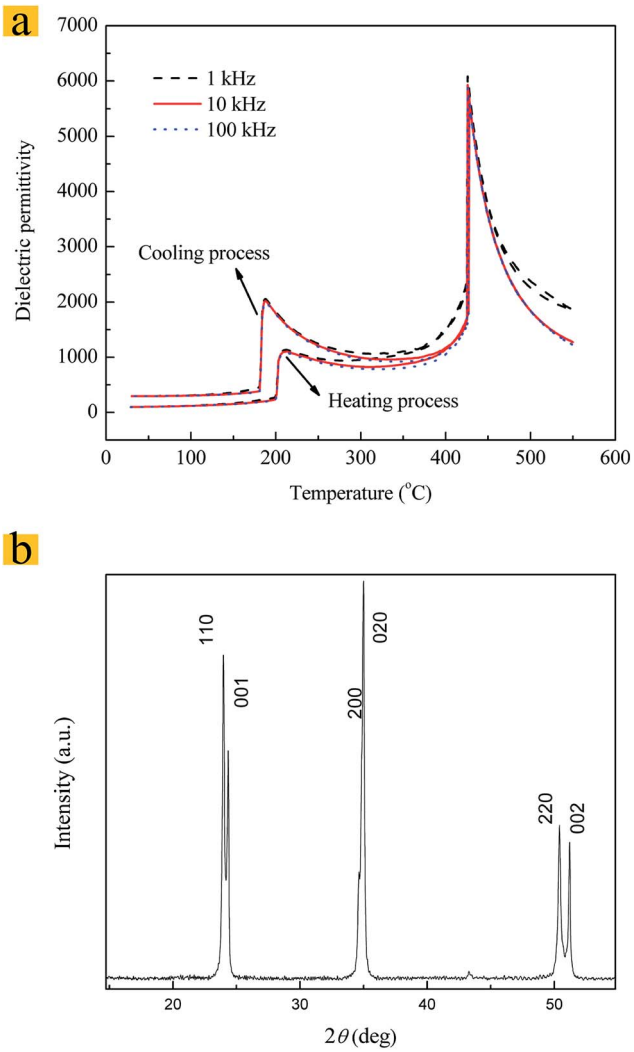

Fig. 2 (a) Temperature dependence of dielectric constants for heating and cooling processes. (b) X-ray powder diffraction patterns of the KNN47 single crystal.

Silver electrodes were painted on the two desired surfaces of each sample, and the samples were poled under an electric field of 100–200 V mm^{-1} at 180 °C. Combined resonance/anti-resonance and ultrasonic methods were used to retrieve the 11 independent constants, allowing the determination of these coefficients with a high degree of self-consistency. In the resonance and anti-resonance frequency method, the electromechanical coupling factors, k_{15}, k_{31}, k_{33}, k_t, piezoelectric strain constants, d_{31}, d_{33}, and elastic compliance constants, s_{11}^E, s_{11}^D, s_{33}^E, s_{33}^D, were calculated with an Agilent, E4294A impedance-phase analyzer. The free and clamped dielectric constants, ε_{11}^T, ε_{33}^T, ε_{11}^S, ε_{33}^S, were determined from low- and high-frequency capacitance measurements. In ultrasonic measurements, a cube of sample (1.2 mm edge length) with orientation $[001]_C \times [010]_C \times [100]_C$ was used by a 15 MHz longitudinal wave transducer and a 20 MHz shear wave transducer (Panametrics Com.). Five elastic stiffness constants, c_{11}^E, c_{44}^E ($=c_{55}^E$), c_{66}^E, c_{33}^D, c_{44}^D ($=c_{55}^D$), and c_{66}^D, can be deduced from the phase velocities of the longitudinal and shear waves

Table 1 Complete set of material constants of $[001]_C$-poled KNN47 single crystal, compared to those of KNN80 (ref. 20) and KNNT single crystal (ref. 21)[a]

Elastic stiffness constants: C_{ij}^E and C_{ij}^D (10^{10} N m^{-2})

Material	C_{11}^E	C_{12}^E	C_{13}^E	C_{33}^E	C_{44}^E	C_{66}^E	C_{11}^D	C_{12}^D	C_{13}^D	C_{33}^D	C_{44}^D	C_{66}^D
KNN47	22.2	18.3	4.6	6.7	7.7	7.16	24.1	20.2	1.1	13.3	7.8	7.16
KNN80	27.4	15.0	6.2	14.6	7.9	8.5	28.3	15.9	3.0	26.4	9.1	8.5
KNNT	17.2	11.0	10.2	13.8	8.3	9.3	22.9	16.8	2.8	23.2	8.9	9.3

Elastic compliance constants: s_{ij}^E and s_{ij}^D (10^{-12} N m^{-2})

Material	S_{11}^E	S_{12}^E	S_{13}^E	S_{33}^E	S_{44}^E	S_{66}^E	S_{11}^D	S_{12}^D	S_{13}^D	S_{33}^D	S_{44}^D	S_{66}^D
KNN47	14.3	−11.4	−2.0	17.6	13.0	14.0	14.0	−11.7	−0.2	7.5	12.8	14.0
KNN80	5.4	−2.7	−1.2	7.9	12.7	12.0	5.2	−2.9	−0.3	3.9	11.0	12.0
KNNT	11.9	−4.3	−5.6	15.5	12.0	10.7	9.4	−6.8	−0.3	4.4	11.2	10.7

Piezoelectric coefficients: $e_{i\lambda}$ (C m^{-2}), $d_{i\lambda}$ (10^{-12} C N^{-1}), $g_{i\lambda}$ (10^{-3} Vm N^{-1}), and $h_{i\lambda}$ (10^8 V m^{-1})

Material	e_{15}	e_{31}	e_{33}	d_{15}	d_{31}	d_{33}	g_{15}	g_{31}	g_{33}	h_{15}	h_{31}	h_{33}
KNN47	4.6	−5.9	11.1	60	−40	220	3.1	−8.3	46	2.4	−31.5	59.3
KNN80	7.4	−3.4	12.3	93.7	−23.2	104.2	27.1	−8.4	37.6	13.4	−26.6	97.1
KNNT	3.7	−5.2	6.7	45	−77	162	17.4	−32.6	68.5	15.5	−110.0	140.0

Relative dielectric constants: ε (ε_0), β (10^{-4} $\varepsilon_0{}^{-1}$)

Material	ε_{11}^T	ε_{33}^T	ε_{11}^S	ε_{33}^S	β_{11}^T	β_{33}^T	β_{11}^S	β_{33}^S
KNN47	2194	540	2162	211.4	4.56	18.5	4.63	47.3
KNN80	390	313	320	141	25.6	31.9	31.2	70.9
KNNT	291	267	272	54	34.4	37.5	36.8	186

Electromechanical coupling coefficient: k

Material	k_{15}	k_{31}	k_{33}	k_t
KNN47	0.120	0.151	0.759	0.702
KNN80	0.45	0.19	0.706	0.67
KNNT	0.234	0.46	0.827	0.646

[a] $\rho = 4.412 \times 10^3$ kg m^{-3}.

measured along $[001]_C$, $[010]_C$, $[100]_C$, respectively. The density of the samples was determined by applying Archimedes' principle.

Results and discussion

Fig. 2a shows the temperature dependence of the dielectric constants of $[001]_C$-oriented KNN47 single crystals for heating and cooling processes. It can be seen that the dielectric constants exhibit two anomalies in both the heating and cooling process. The anomalies occurred at approximately 205 °C and 428 °C for the warming process and 186 °C and 425 °C for the cooling process. These values correspond to the orthorhombic–tetragonal phase transition temperature, T_{O-T}, and the tetragonal–cubic phase transition temperature, T_C, respectively. The differences between T_{O-T} and T_C for the heating and cooling processes are approximately 19 °C and 3 °C, respectively. The orthorhombic phase structure is demonstrated from the power XRD pattern of a KNN47 single crystal, exhibiting the typical perovskite structure of an orthorhombic phase, as shown in Fig. 2b. These data show that the KNN47 single crystals exhibit an orthorhombic phase structure at room temperature and, as T_{O-T} is far from room temperature, the properties can be determined reliably.

The complete set of elastic, piezoelectric, and dielectric constants for the $[001]_C$-poled KNN47 single crystal are listed in Table 1, where they are compared to those of KNN80 and KNNT single crystals.[20,22] The density was determined to be 4.412×10^3 kg m^{-3}. The d_{33}, d_{31}, d_{15} values, which were measured using the resonance method, are 220 pC N^{-1}, −40 pC N^{-1}, and 60 pC N^{-1} along $[001]_C$, respectively. The measured k_t, k_{33}, k_{31}, k_{15} were 0.702, 0.759, 0.151, 0.120, respectively. It is of particular interest that the elastic stiffness constants of the KNN47 single crystal are much smaller than those of the KNN80 single crystal, except for C_{12}^E and C_{12}^D. By contrast, the elastic compliance constants are much larger than those of a KNN80 single crystal, except for S_{12}^E, S_{13}^E, S_{12}^D and S_{13}^D. Among them, S_{11}^E and S_{33}^E in KNN47 single crystals are over 2 times greater than those in KNN80 single

crystals, which strongly indicates a greater transverse mechanical adaptability along the $[100]_C$ and $[001]_C$ direction. The KNN47 single crystal also exhibits high transverse dielectric constants, with $\varepsilon_{11}^T = 2194$ and $\varepsilon_{11}^S = 2162$. These are much higher than the longitudinal dielectric constant, $\varepsilon_{33}^T = 540$, and the transverse dielectric constants seen in other materials.[20–23] In comparison to the electromechanical coupling coefficient in KNN80 single crystal, k_t and k_{33} in KNN47 are significantly greater, while k_{31} and k_{15} are reduced. The impedance spectrum of electromechanical coupling coefficient, k_t, which is calculated from the formula: $k_t = \frac{\pi}{2}\frac{f_r}{f_a}\tan\left(\frac{\pi}{2}\frac{f_a - f_r}{f_a}\right)$, where f_r and f_a represent the resonant and anti-resonant frequencies, is shown in Fig. 3.

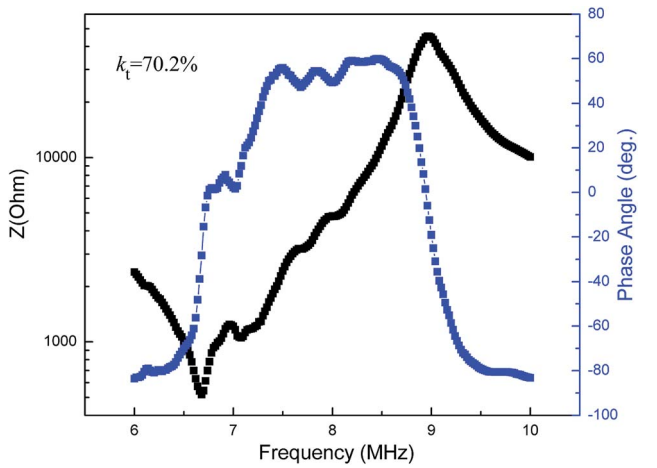

Fig. 3 The impedance and phase angle spectra of KNN47 single crystal.

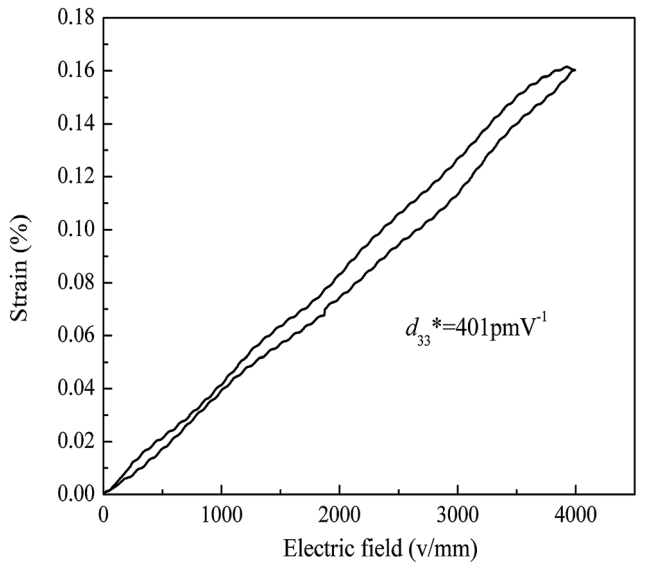

Fig. 4 Strain *vs.* unipolar electric field of the KNN47 single crystal at 1 Hz.

Fig. 4 shows the dependence of the unipolar strain on the applied electric field of KNN47 single crystals, under a maximum electric field of 4 kV mm^{-1}. The curve exhibits a small hysteresis with the measurement frequency of 1 Hz. The maximum strain of 0.16%, and corresponding piezoelectric coefficient, d_{33}^*, of 401 pm V^{-1}, derived from the slope of the strain–field curve, were obtained when the electrical field reached 4 kV mm^{-1}. The large value of d_{33}^*, which is much higher than that measured *via* the resonance method (220 pC N^{-1}) and Berlincourt method (250 pC N^{-1}), is likely due to the morphotropic phase boundary around $x = 0.5$. A brief comparison of the properties of KNN based materials is made in Table 2. The value of d_{33}^* is much higher than those reported in ref. 24 and 25. At this time, the electromechanical coupling coefficient, $k_t = 0.702$, is the highest of any reported in the literature for KNN-based materials.

Conclusion

In summary, we have grown a large-sized, high-quality KNN47 single crystal using the top seeded solution growth method. In order to better understand the properties of KNN47 single crystal, a complete set of elastic, dielectric, and piezoelectric constants for a $[001]_C$-poled KNN47 single crystal has been determined *via* combined resonance and ultrasonic methods. The $[001]_C$-poled KNN47 single crystal exhibits a large piezoelectric coefficient ($d_{33} = 220$ pC N^{-1}, which is the highest in pure KNN materials), high electromechanical coupling coefficients ($k_{33} = 0.759$ and $k_t = 0.702$, which are at the highest range), high dielectric constants ($\varepsilon_{11}^T = 2194$ and $\varepsilon_{11}^S = 2162$), and relatively high elastic compliance constants ($S_{11}^E = 14.3 \times 10^{-12}$ N m^{-2} and $S_{33}^E = 17.6 \times 10^{-12}$ N m^{-2}). Furthermore,

Table 2 Comparison of the properties of KNN based materials

Materials	d_{33} (pC N^{-1})	k_t (%)	k_{33} (%)	ε_{33}^T (ε_0) (1 kHz)	T_C (°C)	Ref.
KNN47	220[a], 250[b], 401[c]	70.2	75.9	540	428	This work
KNN80	104.2[a], 110[b]	67	70.6	313	455	20
KNNT	162[a], 200[b]	64.6	82.7	267	291	21
Mn-doped KNN	161[b]	—	64	424 (10 kHz)	407	26
KNN	160[b]	45	—	240	393	16
0.95KNN–0.05LiNbO$_3$	405[b]	61	—	185	426	18
KNN47	110[c]	—	—	600	390	24
LF4T	416[a], 750[c]	61 (k_p)	—	1570	253	5
PZT4	410[b], 700[c]	60 (k_p)		2300	250	5

[a] Determined by resonance method. [b] Measured by d_{33} meter. [c] Calculated from the slope of high field strain curve.

a large electrical field induced strain of 0.16% was measured. The piezoelectric coefficient, d^*_{33}, was measured to be as high as 401 pm V^{-1}, likely arising due to the morphotropic phase boundary around $x = 0.5$. These excellent properties make this KNN47 single crystal an ideal candidate for application as a high-performance transducer material.

Acknowledgements

This work was supported by the National Natural Science Foundation of China (Grant No. 50902034, 11074059, and 61205011), the Science Fund for Distinguished Young Scholars of Heilongjiang Province (Grant No. JC200710), and the Program for Innovation Research of Science at the Harbin Institute of Technology (No. B201504). The authors wish to thank the Laboratory of Micro-Optics and Photonic Technology of Heilongjiang Province for help with the experiments.

References

1 Q. M. Zhang, H. Wang, N. Kim and L. E. Cross, *J. Appl. Phys.*, 1994, **75**, 454–459.
2 C. He, X. Z. Li, Z. J. Wang, Y. Liu, D. Q. Shen, T. Li, X. F. Long and Z. G. Ye, *CrystEngComm*, 2012, **14**, 4513–4519.
3 Y. Liu, X. Z. Li, Z. J. Wang, C. He, T. Li, L. D. Ai, T. Chu, D. F. Pang and X. F. Long, *CrystEngComm*, 2013, **15**, 1643–1650.
4 R. M. Fernando, D. C. Adolfo, L. J. Rigoberto, J. R. Juan and F. F. José, *J. Mater. Chem.*, 2012, **22**, 9714.
5 Y. Saito, H. Takao, T. Tani, T. Nonoyama, K. Takatori, T. Homma, T. Nagaya and M. Nakamura, *Nature*, 2004, **432**, 84–87.
6 E. Hollenstein, M. Davis, D. Damjanovic and N. Setter, *Appl. Phys. Lett.*, 2005, **87**, 182905.
7 J. Rodel, W. Jo, K. T. P. Seifert, E.-M. Anton, T. Granzow and D. Damjanovic, *J. Am. Ceram. Soc.*, 2009, **92**, 1153.
8 K. Wang, F.-Z. Yao, W. Jo, D. Gobeljic, V. V. Shvartsman, D. C. Lupascu, J.-F. Li and J. Rodel, *Adv. Funct. Mater.*, 2013, **23**, 4079.
9 H. Deng, X. Y. Zhao, H. W. Zhang, C. Chen, X. B. Li, D. Lin, B. Ren, J. Jiao and H. S. Luo, *CrystEngComm*, 2014, **16**, 2760.
10 V. J. Tennery and K. W. Hang, *J. Appl. Phys.*, 1968, **39**, 4749–4753.
11 B. P. Zhang, J. F. Li, K. Wang and H. Zhang, *J. Am. Ceram. Soc.*, 2006, **89**, 1605–1609.
12 M. Ahtee and A. M. Glazer, *Acta Crystallogr.*, 1976, **32**, 434–446.
13 L. Egerton and D. M. Dillon, *J. Am. Ceram. Soc.*, 1959, **42**, 438–442.
14 G. H. Haertling, *J. Am. Ceram. Soc.*, 1967, **50**, 329–330.
15 L. Wu, J. L. Zhang, C. L. Wang and J. C. Li, *J. Appl. Phys.*, 2008, **103**, 084116.
16 D. Lin, Z. Li, S. Zhang, Z. Xu and X. Yao, *Solid State Commun.*, 2009, **149**, 1646–1649.
17 H. Tian, C. Hu, X. Meng, P. Tan, Z. Zhou, J. Li and B. Yang, *Cryst. Growth Des.*, 2015, **15**, 1180.
18 K. Chen, G. S. Xu, D. F. Yang, X. F. Wang and J. B. Li, *J. Appl. Phys.*, 2007, **101**, 044103.
19 H. Ursic, A. Benĉan, M. Skarabot, M. Godec and M. Kosec, *J. Appl. Phys.*, 2010, **107**, 033705.
20 H. Tian, C. Hu, X. Meng, Z. Zhou and G. Shi, *J. Mater. Chem. C*, 2015, **3**, 9609–9614.
21 L. Zheng, X. Huo, R. Wang, J. Wang, W. Jiang and W. Cao, *CrystEngComm*, 2013, **15**, 7718–7722.
22 B. Jaffe, W. R. Cook and H. Jaff, *Piezoelectric Ceramics*, Academic, New York, 1971.
23 D. A. Berlincourt, D. R. Curran and H. Jaffe, *Physical Acoustics: Principle and Methods*, Academic, New York, 1964.
24 Y. Kizaki, Y. Noguchi and M. Miyayama, *Key Eng. Mater.*, 2007, **350**, 85–88.
25 F. Z. Yao, K. Wang and J. F. Li, *J. Appl. Phys.*, 2013, **113**, 174105.
26 Y. Inagaki and K. I. Kakimoto, *Appl. Phys. Express*, 2008, **1**, 061602.